Regenerative Therapy 29 (2025) 282–291

Contents lists available at ScienceDirect

Regenerative Therapy

journal homepage: http://www.elsevier.com/locate/reth

Original Article

Fabrication of gelatine/fucoidan nanogel-coated silver nanoparticles for the treatment of wound healing therapy and nursing care

Jiao Hao [a], Xiaozhen Liu [b], Yaomiao Du [a, *]

[a] Department of Emergency, Shanxi Norman Bethune Hospital, Taiyuan 030032, China
[b] Department of Interventional Therapy for Tumors and Vascular Diseases, Shanxi Norman Bethune Hospital, Taiyuan 030032, China

ARTICLE INFO

Article history:
Received 20 January 2025
Received in revised form
26 February 2025
Accepted 9 March 2025

Keywords:
Antibacterial
Biopolymer
Gelatine
Fucoidan
Silver nanoparticles
Wound healing

ABSTRACT

Microbial infections and tissue damage by dressing removal are common problems in wound healing. In this study, gelatine/fucoidan nanogel coated with silver nanoparticles (Ag@Gel/Fu) by simple polymerization technique to assess the antibacterial potential Against human infectious pathogens and wound healing activity Against L929 fibroblast cells. The incorporation of silver nanoparticles in Ag@Gel/Fu nanogel was confirmed by UV–vis, XRD, and SEM analysis techniques. The results of the antibacterial assay revealed that the Ag@Gel/Fu nanogel showed excellent bacterial growth reduction and zone of inhibition against *Escherichia coli* and *Staphylococcus aureus*, depending upon the concentrations. In vitro wound healing results exhibit rapid regeneration of L929 cells in a short duration. It has more advantages, such as Ag@Gel/Fu, to prevent damage to outer skin tissue by infections. It is the more significant bacterial and biofilm infection control of the wound sites. The overall results confirmed that coating of biopolymer and marine polysaccharide fucoidan enhances the biological property of Ag@Gel/Fu nanogel and wound healing potential. Ag@Gel/Fu nanogel co-culture with fibroblast cells showed no cytotoxic effect after 48 h. Finally, Ag@Gel/Fu nanogel is an effective material for infected wound healing nursing care applications.

1. Introduction

Polymicrobial colonization is the most frequent pathogenic in wounds, leading to a severe infection risk. In the period of microbial infection, the wound-healing process is very complicated and develops chronicity [1–4]. The patients suffer from trauma, high costs of treatment, and failure of wound management practices. The challenges of the wound healing process, like expensive drugs and repair materials, can cause an economic and public health burden. The self-healing methods of skin tissues can be disrupted, and wound healing is hindered by toxic substances generated by skin microbes and external factors [5–8]. The therapeutic value and utilization of topical antibiotics and antiseptics in managing nonhealing, noninfected wounds are highly contentious. The appropriate systemic antibiotics have been suggested to be essential in managing nonhealing, chronically infected wounds [9–11].

A wound dressing is to meet multiple demands to promote successful recovery. It must be both non-toxic and effective in opposition to microbes, preserve moist wounds, provide mechanical defense, permit gas exchange, and accelerate the process of wound healing [12–16]. The most important among these is the antibacterial operation, which keeps wounds free from bacteria and promotes a rapid healing process. Infections with bacteria remain possible even if a dressing covers a wound due to the moist atmosphere, which allows bacteria to grow and nurture themselves [17–20]. Utilizing nanoparticles to control wound infections is the most advanced and efficient strategy. Silver is unique, unlike other nanoparticles, due to its size and positive surface charge, which is easily attracted by the negatively charged bacterial cell membrane. They can adhere to bacterial cell walls, and dysfunctions in the respiratory mechanism can cause bacterial cell death [21–26].

Recently, surface coating and covalent crosslinking of biopolymers with silver nanoparticles is a new strategy to improve the bioactivity of Ag nanoparticles against human diseases [27–29].

* Corresponding authors. No. 99 Longcheng Street, Taiyuan 030032, Shanxi Province, China.
E-mail address: 15234177060@163.com (Y. Du).

Peer review under responsibility of the Japanese Society for Regenerative Medicine.

https://doi.org/10.1016/j.reth.2025.03.001

Polysaccharides extracted from marine resources are promising matrix materials utilized in therapeutics. These polysaccharides show various pharmacological effects, such as anticancer, wound healing, antibacterial, antioxidant properties, and biocompatibility [30–33]. Fucoidan (Fu), a sulfated polysaccharide derived from marine microalgae, primarily consists of sulfated L-fucose, with varying proportions of D-glucuronic acid, arabinose, glucose, D-galactose, L-rhamnose, D-xylose, and D-mannose, contingent upon the specific species of brown seaweed [34]. The natural, non-toxic, and biodegradable biopolymer Fu demonstrates diverse bioactive capabilities, including anti-inflammatory, bone regeneration, wound healing, antioxidant, and antitumorigenic effects [35]. Fu suppresses proinflammatory cytokines and positively enhances the production of anti-inflammatory cytokines to expedite the wound healing process. Furthermore, metallic nanoparticles have garnered considerable attention in bioenergy, environmental, and biomedical research [36]. Notably, green-synthesized silver nanoparticles facilitate wound healing by preventing bacterial infections, while the capping agents function as anti-inflammatory agents [37].

Gelatin is a by-product of fish skin collagen, denatured only in acidic and heating conditions. It is a promising polymer in biomedicine because of its stability, biocompatibility, and biodegradability [38–41]. In addition, fucoidan is a sulfated polysaccharide derived from marine seaweeds that exhibits antitumor, immunomodulatory, antimicrobial, and antioxidant efficacies owing to its sulfate groups [42–44]. In this study, we fabricated gelatin and fucoidan dual bio polysaccharides incorporated silver nanoparticles for microbial infection control and wound healing nursing care applications. In the future, it might be a suitable bioactive material for treating infected wounds.

2. Material and methods

2.1. Materials

Glacial acetic acid, silver nitrate (NO_3), methanol, Gelatin (porcine skin, type A), crystal violet, and tryptic soy broth (TSB) were purchased from Sigma-Aldrich Co., USA. Mueller-Hinton Agar, nutrient broth, and sterile disc were obtained from Hi-Media, China. Pathogens, such as *Staphylococcus aureus* ATCC 25913 and *Escherichia coli* ATCC 9028, were collected from the American Type Culture Collection.

2.2. Preparation of Ag@Gel/Fu nanogel

The nanogel preparation was carried out using the previous methodology of Froelich et al., with some modifications [23]. Briefly, gelatin and solution 2 wt % were prepared by dissolving low molecular weight gelatine power in DD water under magnetic agitation at 300 rpm at 40 °C for 2 h. Then, 20 mg of fucoidan powder was added to the gelatine solution, and the stirring continued for another 1 h. Finally, silver nitrate solution 1 wt % was slowly added into gelatine, and fucoidan solution was stirred at 500 rpm speed at room temperature for 1 h. The colloids were washed by centrifugation. The Ag@Gel/Fu nanogel was stored in the refrigerator for further use.

2.3. FT-IR analysis

The characteristic functional groups of Ag@Gel/Fu nanogel were identified by FT-IR spectroscopy, PerkinElmer, Llantrisant, UK. The infrared spectrum was recorded at an average range of 1 cm^{-1} from 400 to 4000 cm^{-1} wavenumber.

2.4. SEM analysis

The Ag@Gel/Fu nanogel was gold sputter coated and dried for 24 h for observing scanning electron microscopy (SEM- S4800, Hitachi, Japan.) at 20 kV. The surface morphology of fabricated Ag@Gel/Fu nanogel was observed under different Ag@Gel/Fu magnifications, and images were captured.

2.5. Bacterial culture

Wound-infecting bacterial strains *Staphylococcus aureus* (ATCC 6538) and *Escherichia coli* (ATCC 25922) were collected from Shanghai BioRc Co., Ltd. Shanghai, China. Bacteria strains were cultured at 37 °C an orbital shaker in an LB medium. The total count of bacterial cells was maintained at 108 CFU/mL. The bacteria-loaded agar culture plates were incubated at 37 °C under 5 % CO_2 flow.

2.6. Antibacterial activity by well diffusion assay

The antibacterial potential of Ag@Gel/Fu nanogel was examined using the Agar diffusion method against skin infectious pathogens *S. aureus* and *E. coli*. Approximately 50 μL of the bacteria was swabbed on the surface of the Agar plates. The wells were created by using 1 mL micro tips. Then, the different concentration (25–100 μg/mL) of Ag@Gel/Fu nanogel was loaded into wells. The nanogel-treated agar petri dishes were incubated at 37 °C for 12 h. After the treatment, the zone of inhibition was calculated using an antimicrobial scale of millimeters.

2.7. Plate count assay

The micro-dilution method examined the antibacterial efficacy of Ag@Gel/Fu nanogel against *Escherichia coli* and *Staphylococcus aureus*. About 100 μL of Ag@Gel/Fu nanogel was uniformly mixed with 900 μL of bacterial culture. The culture medium was maintained in an orbital shaker at 120 rpm speed under 37 °C for 12 h. Further, PBS (pH~7.4) was utilized to dilute the microbial solutions to make 105 CFU/mL^{-1} concentration. Approximately 30 μL of bacterial culture was added in the center place of agar plates and uniformly swabbed by an L-rod glass. The Ag@Gel/Fu nanogel-loaded agar plates were incubated for another 24 h at 37 °C. Finally, the Ag@Gel/Fu nano gel-treated plate was observed, and the Nikon camera was used to take photographs. The bacterial colonies were counted using Image J software.

2.8. Anti-biofilm activity

The biofilm inhibitory efficacy of Ag@Gel/Fu nanogel was assessed against wound-infecting bacterium MRSA and *E. coli* based on the protocol of Prabhu et al. [45]. The bacterial strains were dispersed 108 CFU/mL in TSB medium with 0.5 % glucose in the presence of Ag@Gel/FUu nanogel (25–100 μg/mL) and incubated under 37 °C for 48 h. Then, treatment the contents of the wells were discarded and washed many times with PBS solution. Biofilm-formed bacteria were fixed with 2 % sodium acetate. Bacteria-coated microscopic slides were stained with 1 mL of 0.5 % crystal violet solution. The unwanted stain was removed by washing DD water. Stained biofilms were fated by 10 % glacial acetic acid treatment for 10 min. The absorbance of the biofilm was quantified using an ELISA plate reader at 570 nm.

2.9. Biocompatibility of Ag@Gel/Fu nanogel

Skin fibroblast cells (L929) were used to examine the biocompatibility of nanogel. The MTT cell viability assay was utilized to investigate the cytotoxic effect of Ag@Gel/Fu nanogel. The L929 cells are sub-cultured in 96-well plates with DMEM containing 10 % of FBS and treated with Ag@Gel/Fu nanogel with various concentrations (10–100 μg/mL) after the uniform cell proliferation. The wells with PBS solution were considered the control. The nano gel-treated cells were incubated for 24 h at 37 °C, with an underflow of 5 % CO_2. Then, 20 μL of MTT solution was added into each well and incubated again for 4 h. After the attachment of the MTT stain, the excess medium was removed by 100 μL DMSO solution using microcentrifugation. The total amount of cell viability was calculated from the optical density (OD) of the medium at the wavelength of 595 nm. This formula quantified the percentage of cell viability.

$$\%\ of\ cell\ viability = \frac{OD\ value\ of\ treatment}{OD\ value\ of\ control} X\ 100$$

The morphological changes and cytotoxicity of Ag@Gel/Fu nanogel-treated L929 cells were examined by fluorescence microscopic imaging. Cells were treated with the IC_{50} concentration of Ag@Gel/Fu, fucoidan, and Gel/Fucoidan and incubated for 24 h at 37 °C under CO_2 flow. Then, an AO/EB dual stain solution of 100 μL was added and maintained at optimum conditions. The deformities and dead cells were visualized under fluorescence microscopy at various time intervals (1, 3, and 5 days), and images were captured on alternative days.

2.10. In vitro wound scratch assay

The wound healing efficacy of Ag@Gel/Fu nanogel was evaluated by *in vitro* wound scratch assay against L929 cells. The cells (5×10^5) were pre-seeded and cultured overnight at 37 °C under CO_2 flow. After the sub-culture, cells were rinsed with PBS solution. A sterile microtip (200 μL) was utilized to create a wound scratch among the cells in each well. The unwanted media and cell debris were discarded by washing with PBS solution. Then, the cells were treated with 30 μg/mL of Ag@Gel/Fu nanogel and incubated at 37 °C. The cytological changes, cell proliferation, and migration were observed, and an inverted phase contrast microscope captured images. The percentage of the wound closer was analyzed by Adobe Photoshop software and recorded at ultimate time intervals. The fluorescent microscopic images were taken after DAPI staining.

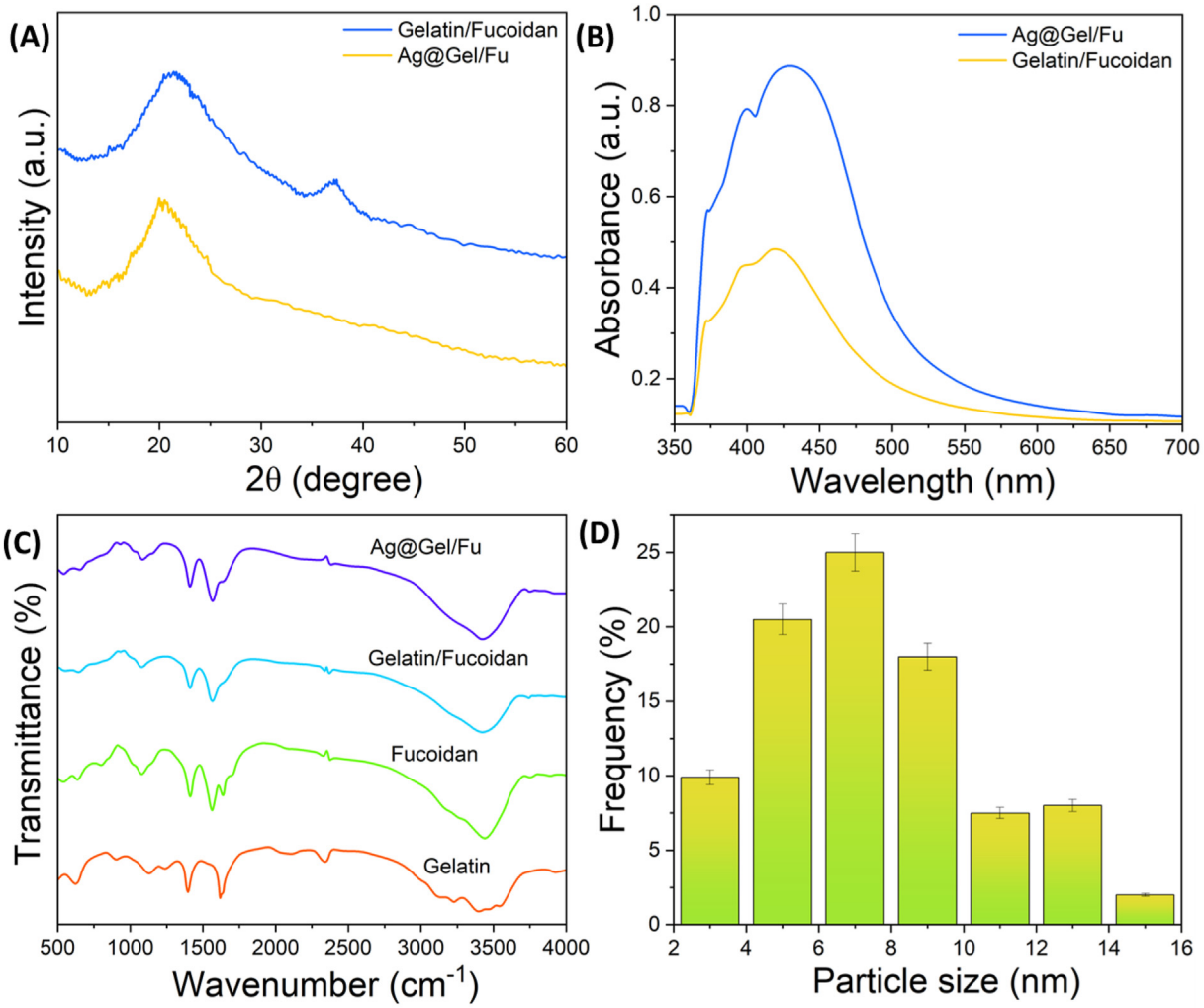

Fig. 1. **(A)** XRD spectra of Gelatin/Fucoidan gel and Ag@Gel/Fu, **(B)** UV–vis spectra of Gelatin/Fucoidan gel and Ag@Gel/Fu, **(C)** FTIR spectra of gelatin (black), Fucoidan, Gelatin/Fucoidan gel, and Ag@Gel/Fu. (D) DLS analysis of Ag/Gel/Fu nanogel. Data were stated as means ± SEM (n = 3).

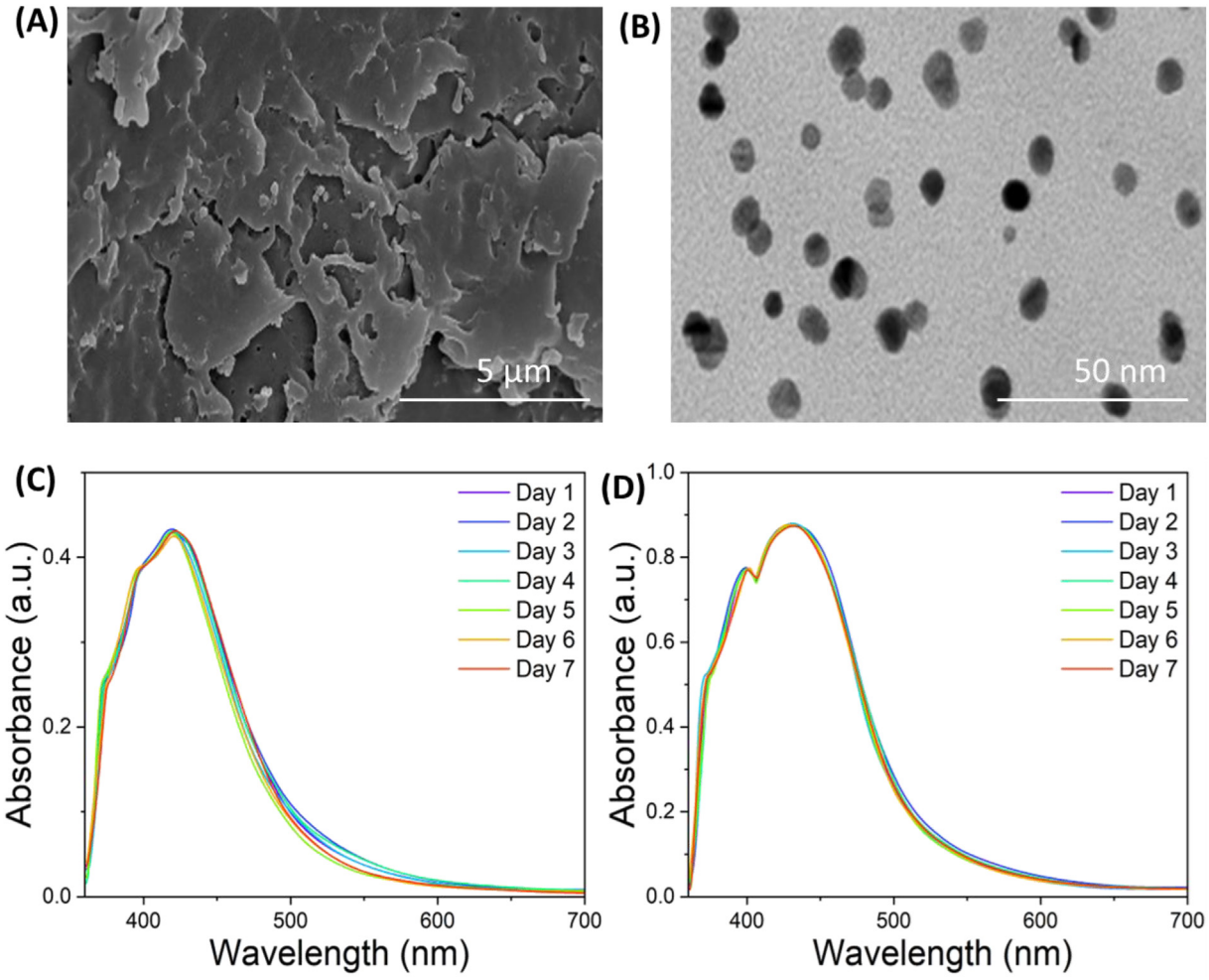

Fig. 2. **(A)** High-resolution scanning electron microscopy (HR-SEM) and **(B)** High-resolution Transmission electron microscopic (HR-TEM) images of Ag@Gel/Fu nanogel. **(C and D)** The stability test of Gelatin/Fucoidan, and Ag@Gel/Fu for 7 days of incubation time.

2.11. Statistical analysis

Students' t-tests were applied to evaluate the significance levels. n.s. denoted not significance; *p < 0.05 represented statistical significance; **p < 0.01 signified moderate statistical significance and ***p < 0.001 represented highly statistical significance.

3. Result and discussion

3.1. XRD analysis of Ag@Gel/Fu nanogel

Ag@Gel/Fu nanogel powder of XRD diffraction patterns has been shown in Fig. 1A. It exhibits a prominent diffraction peak around 23°. Different intensity peaks were established at position $2\theta = 38.26$ in the diffraction X-ray spectrum of Ag@Gel/Fu nanogel, which concurred with the scattering of the silver metallic face-cantered cubic structure (111). The height and purity of the diffraction peak enhanced, increasing the Ag nanoparticle concentration. Additionally, it demonstrates that gelatine can convert Ag + to Ag nanoparticles through XRD investigation.

3.2. UV–vis spectroscopy analysis

Gelatine was utilized as a gelling and stabilizing agent throughout the reduction of Ag@Gel/Fu to increase the homogeneity and stabilization of the silver solution. The solution transformed coloration to a bright yellow after the interaction of silver ions. As Ag@Gel/Fu concentrations increased, the solution's dark color widened, indicating that gelatine effectively reduced Ag@Gel/Fu. In addition, the intensity of the peak in the UV spectroscopy visible range of the nanosilver increased with the rise in Ag@Gel/Fu content. The optical spectrum of Ag@Gel/Fu, as depicted in Fig. 1B, showed a peak at 434, the positive correlation between Ag nanoparticles and gelatin, and the peak intensity indicated Ag@Gel/Fu formation.

3.3. FTIR analysis

The result of FTRI analysis confirmed the successful incorporation of fucoidan within the gelatine biopolymer. The material's extensive nanogel structure resulted from both the chemical crosslinking and the mechanical combining of fucoidan and gelatine. As is observed in Fig. 1C, the amides I, II, and III were identified as the origins for the peaks in the gelatine curve that occurred at 1638 cm^{-1}, 1440 cm^{-1}, and 1239 cm^{-1}. An O–H vibration that stretched at 3478 cm^{-1} additionally culminated in an absorption peak. A substantial amount of deacetylation in fucoidan is indicated through the C–CH_3 deformed vibration peak of absorption at 1407 cm^{-1} and the emergence of amide II at 1560 cm^{-1} for fucoidan. Ag@Gel/Fu nanogel's distinctive peak completely disappeared,

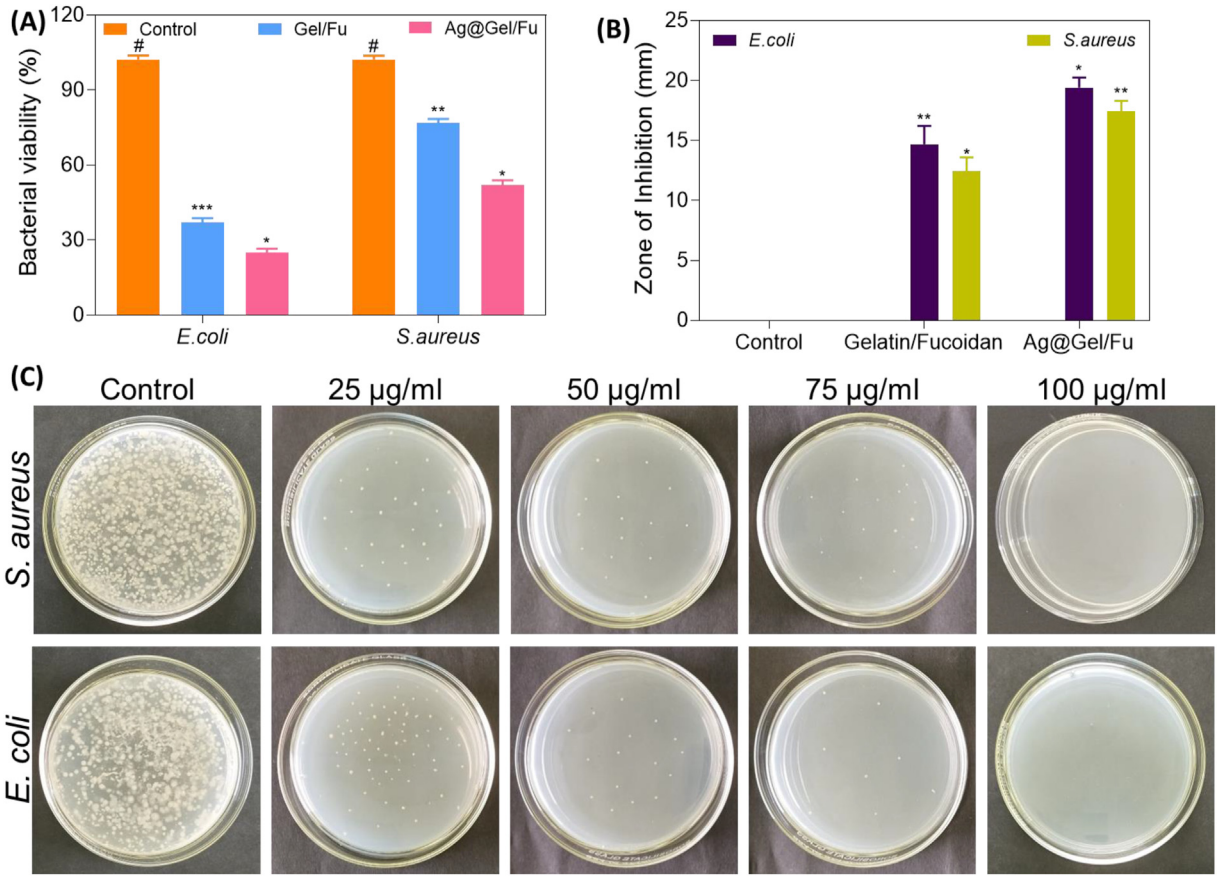

Fig. 3. **(A)** Bacterial growth inhibition of Ag@Gel/Fu against *E. coli* and *S. aureus*. **(B)** Ag@Gel/Fu induced zone of inhibition against *E. coli* and *S. aureus*. **(C)** Antibacterial activity of Ag@Gel/Fu against *E. coli* and *S. aureus* using agar broth dilution assay. Data were stated as means ± SEM (n = 5). *P < 0.05, **P < 0.01, ***P < 0.001, compared with control group (#).

Table 1
Zone of inhibition of human infectious bacterial strains after treatment of AA@ZIF-8 nanocomposite in well diffusion assay.

Microorganism	Zone of inhibition (mm) by the Ag@Gel/Fu nanogel in well diffusion method			
	25 μg/mL	50 μg/mL	75 μg/mL	100 μg/mL
Staphylococcus aureus	6	12	14	16
Escherichia coli	7	9	12	15

but amide III shifted to a wider band, indicating that chemical interactions had bound gelatine and fucoidan. The gelatine hydroxyl group (O—H) is compared with Gelatine/fucoidan, which is present at around 3450 cm^{-1}.

3.4. Morphology and particle size analysis

The morphology and size of Ag@Gel/Fu exhibit an array of physicochemical characteristics. The images of HR-SEM show that

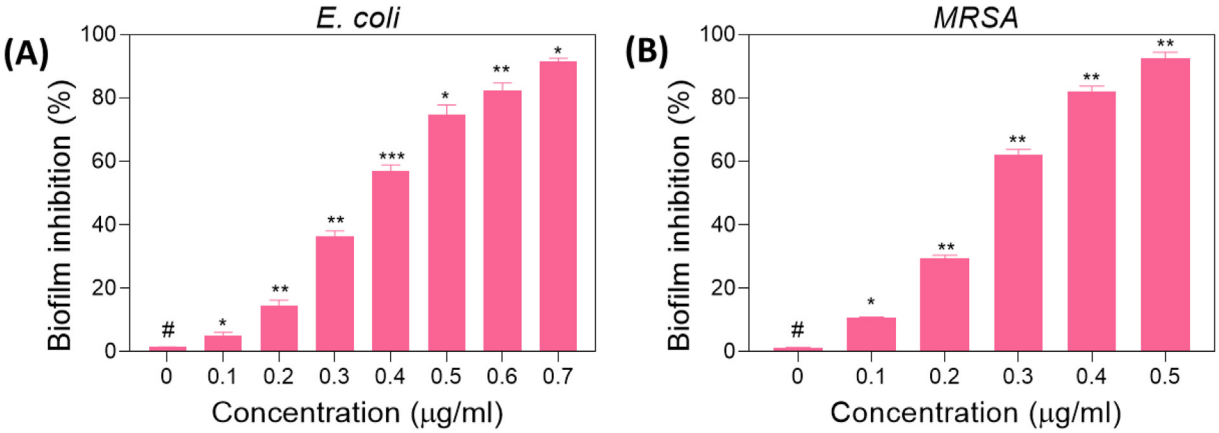

Fig. 4. **(A&B)** Biofilm growth inhibition of *E. coli* and *MRSA* after Ag@Gel/Fu nanogel treatment. Data were stated as means ± SEM (n = 5). *P < 0.05, **P < 0.01, ***P < 0.001, compared with control group (#).

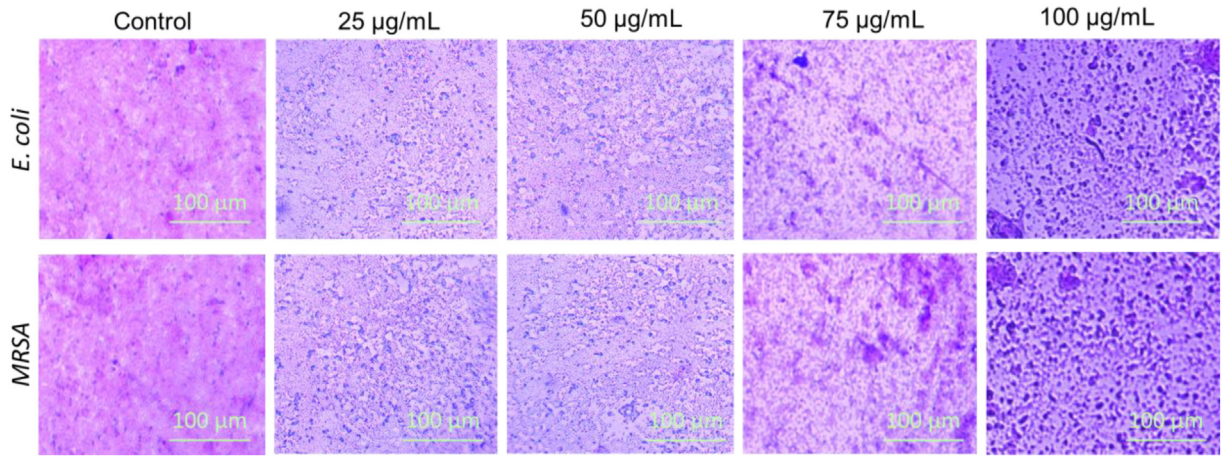

Fig. 5. – Inverted phase contrast microscopic images of *E. coli* and *MRSA* biofilm after treatment of Ag@Gel/Fu in crystal violet assay. The scale bar indicates the 100 μm.

Ag/Gel/Fu nanogel is a sphere-like structure with slight agglomeration (Fig. 2A). TEM images of Ag@Gel/Fu are shown in Fig. 2B. These sample projected images indicate the shape and distribution of their sizes of particles. The constant form of Ag@Gel/Fu and its predominantly 2–10 nm diameter of particles appear in Fig. 2B. In Ag@Gel/Fu nanogel, 77.23 % of the atoms had dimensions between 3 and 6 nm. The polydispersity of 0.155 ± 0.004 and a zeta potential of −28.45 ± 2.78 mV. Ag@Gel/Fu satisfies the necessary dimensions and form factors for effective antimicrobial activity. Ag@Gel/Fu was spread somewhat uniformly. In addition, based on previous studies, the atoms in all three of these samples exhibited a spacing in the lattice of 0.23 nm. DLS analysis (Fig. 1D) indicated that the particle size of the nanogel is 10 nm. Additionally, the nanogel offers promising advantages for effective cellular intake. Due to their ultra-fine particle size and the capability to encapsulate fucoidan, these nanogel are expected to exhibit promising biological functionalities and the ability to cross-control wound pathogens. Further, the storage stability of Gel/Fu and Ag@Gel/Fu nanogels was examined over 7 days at 37 °C, as illustrated in Fig. 2C and D. At 37 °C, the Gel/Fu and Ag@Gel/Fu nanogels exhibited significant stability, with the most intense peak recorded at 434 nm. At 37 °C, the Ag@Gel/Fu nanogel demonstrates its remarkable stability. Conversely, Ag@Gel/Fu nanogel frequently experiences stability challenges stemming from aggregation, oxidation, and the employment of toxic and flammable reducing and stabilizing chemicals, which may compromise nanoparticle stability [46].

3.5. Antibacterial potential of Ag@Gel/Fu nanogel

Bacterial wound infections are the utmost cause of chronicity in humans. The inability of antibiotic drugs to control infections is the main cause of trauma. Bacterial co-infections with influenza virus are the leading cause of human deaths. *Staphylococcus aureus* and *Escherichia coli* infections occur regularly in wounds. The antibacterial activity of Ag@Gel/Fu nanogel against *S. aureus* and *E. coli* is significantly improved in the well diffusion assay. In all concentrations, Ag@Gel/Fu nanogel exhibits the highest zone of inhibitions in both bacterial strains (Fig. 3A&B). The antibacterial activity increased as Ag@Gel/Fu nanoparticle concentration increased (Table 1).

The results of the plate count assay exhibit excellent bacterial growth reduction in a dose-dependent manner. Compared to the alone Gelatin/fucoidan gel, the bacterial growth inhibition of Ag@Gel/Fu nanogel treated groups was three-fold higher (Fig. 3C). The Ag@Gel/Fu nanogel controls bacterial multiplication and enhances cell wall conjugation. This might be explained by the S. aureus cell wall containing more positively charged peptidoglycans. The Ag@Gel/Fu easily penetrates the cell wall region through the

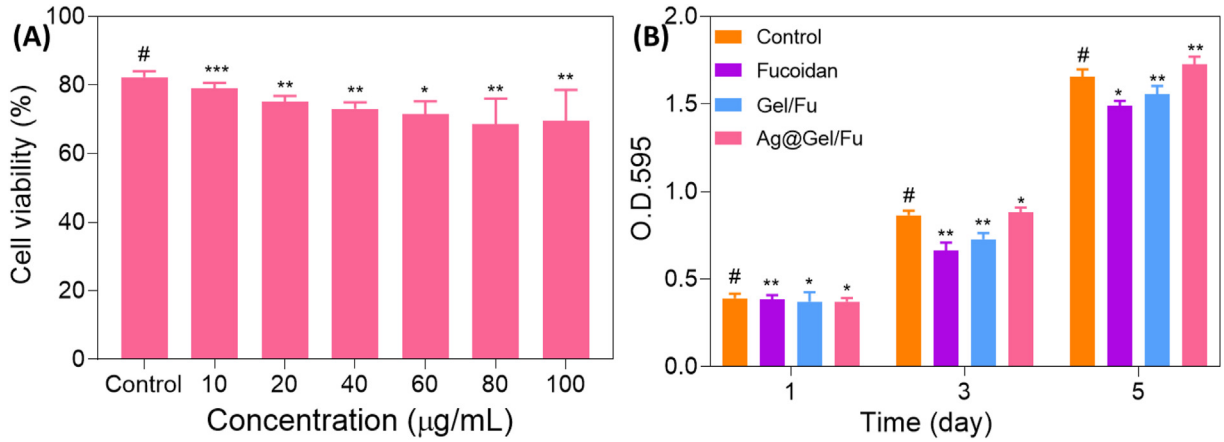

Fig. 6. **(A)** Cytotoxic effect of Ag@Gel/Fu against L929 cells by MTT assay, **(B)** Cell density of L929 cells after nanogel treatment. Data were stated as means ± SEM (n = 5). *P < 0.05, **P < 0.01, ***P < 0.001, compared with control group (#).

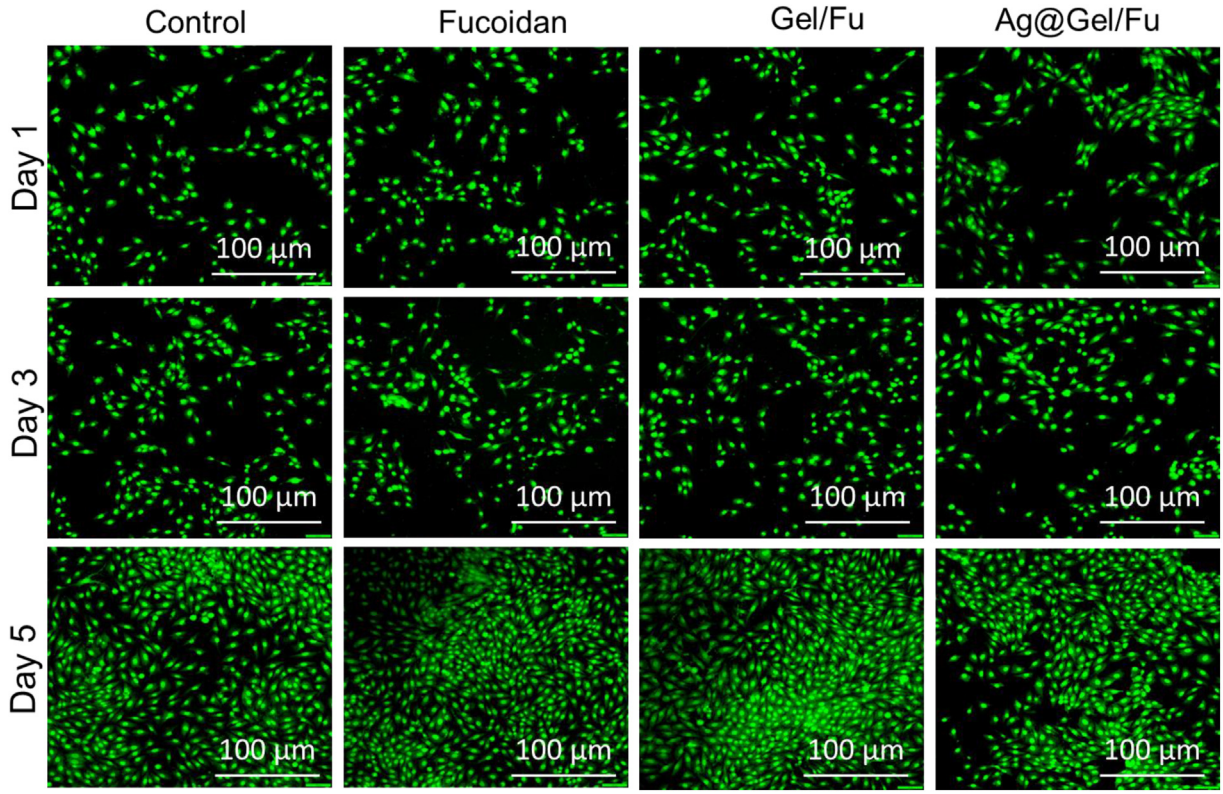

Fig. 7. Fluorescence microscopic images of L929 cells with AO/EB dual staining in biocompatibility assay at various intervals. The scale bar indicates the 100 μm.

electrostatic attraction of silver ions. The nanogel damaged the cell wall structure and destroyed the intercellular organelles. Due to the cell lysis process, the Ag@Gel/Fu nanogel treatment inhibits structural proteins. Releasing positive charged silver ions from Ag@Gel/Fu nanogel leads to cell wall breakages.

3.6. Antibiofilm activity of Ag@Gel/Fu nanogel

Escherichia coli and methicillin-resistant *Staphylococcus aureus* (MRSA) are dangerous pathogens associated with wounds and nosocomial infections, leading to life-threatening disorders. These bacteria significantly contribute to respiratory and wound-related infections, posing considerable challenges in public health management. The biofilm-forming potential of *E. coli* and *MRSA*, along with their resistance to antibiotic therapy, has resulted in failures in wound healing. The antibiofilm properties of Ag@Gel/Fu nanogel were assessed using the crystal violet staining technique. Results indicated that the Ag@Gel/Fu nanogel effectively disrupts biofilm formation by pathogenic bacteria in a concentration-dependent manner. The nanogel-treated *Escherichia coli* and *Staphylococcus aureus* exhibit 78 % and 81 % biofilm growth inhibition, respectively (Fig. 4A&B). The incorporation of fucoidan within the gelatin biopolymer enhances the antibiofilm efficacy of the Ag/Gel composition by weakening the adhesion of *E. coli* and *MRSA* to glass surfaces, thereby preventing biofilm formation. Microscopic examination of control slides showed thick biofilm formations for both strains. In contrast, slides treated with Ag@Gel/Fu nanogel displayed a significant reduction in bacterial growth and damage to biofilm architecture in a dose-dependent manner (Fig. 5). The antibiofilm activity of Ag@Gel/Fu nanogel may be attributed to the synergistic effect of fucoidan and silver ions released from the nanogel. The anti-biofilm efficacy of fucoidan destabilizes the biofilm matrix and causes damage to the bacterial cell wall. Combining silver and fucoidan with the gelatin biopolymer reduces biofilm formation by impairing the quorum-sensing regulatory system. Additionally, silver ions released from Ag@Gel/Fu nanogel hinder bacterial mobility and the production mechanisms of exopolysaccharides. Overall, calorimetric and microscopic studies suggest that Ag@Gel/Fu nanogel may be a promising candidate for wound healing in future public health management.

3.7. Cytotoxicity in vitro

Determining the biocompatibility of materials requires investigating the *in vitro* activity of cells. The bactericidal efficacy of the materials was enhanced as a higher amount of Ag@Gel/Fu nanogel. The cytotoxic effects of Ag@Gel/Fu nanogel have been studied via MTT studies. Separately, the nanogel was mixed with L929 cells for 24 h. Fig. 6A displays an explanation of the experimental outcomes. The cell viability was over 80 % after 24 h, indicating that the Ag@Gel/Fu nanogel was not hazardous to L929 cells. It exhibited promising proliferation of cells, including cell viability of 89.11 ± 2 %, after 48 h respectively. However, few apoptotic cells were observed whether Ag@Gel/Fu in higher concentration. Cell survival and double staining accurately represent the effect of Ag@Gel/Fu nanogel on L929 cells. Following the outcomes of MTT tests, the nanogel encouraged the growth of L929 cells, as shown in Fig. 6B, where the counts of treated cells were very similar to those of the control cells. There was no huge variation in cell death rates across Ag@Gel/Fu nanogel and the control group. The fluorescence images showed no cellular toxic effect and an excellent cell proliferation rate after 5 days. The clear green fluorescence intensity indicates more alive cells after treatment of Ag/Gel/Fu nanogel (Fig. 7). The AO/EB staining experiment confirmed that Ag@Gel/Fu nanogel is safe for fibroblast cells. In the 5 days post-exposure, no notable cell wall damage and shrinkage appear.

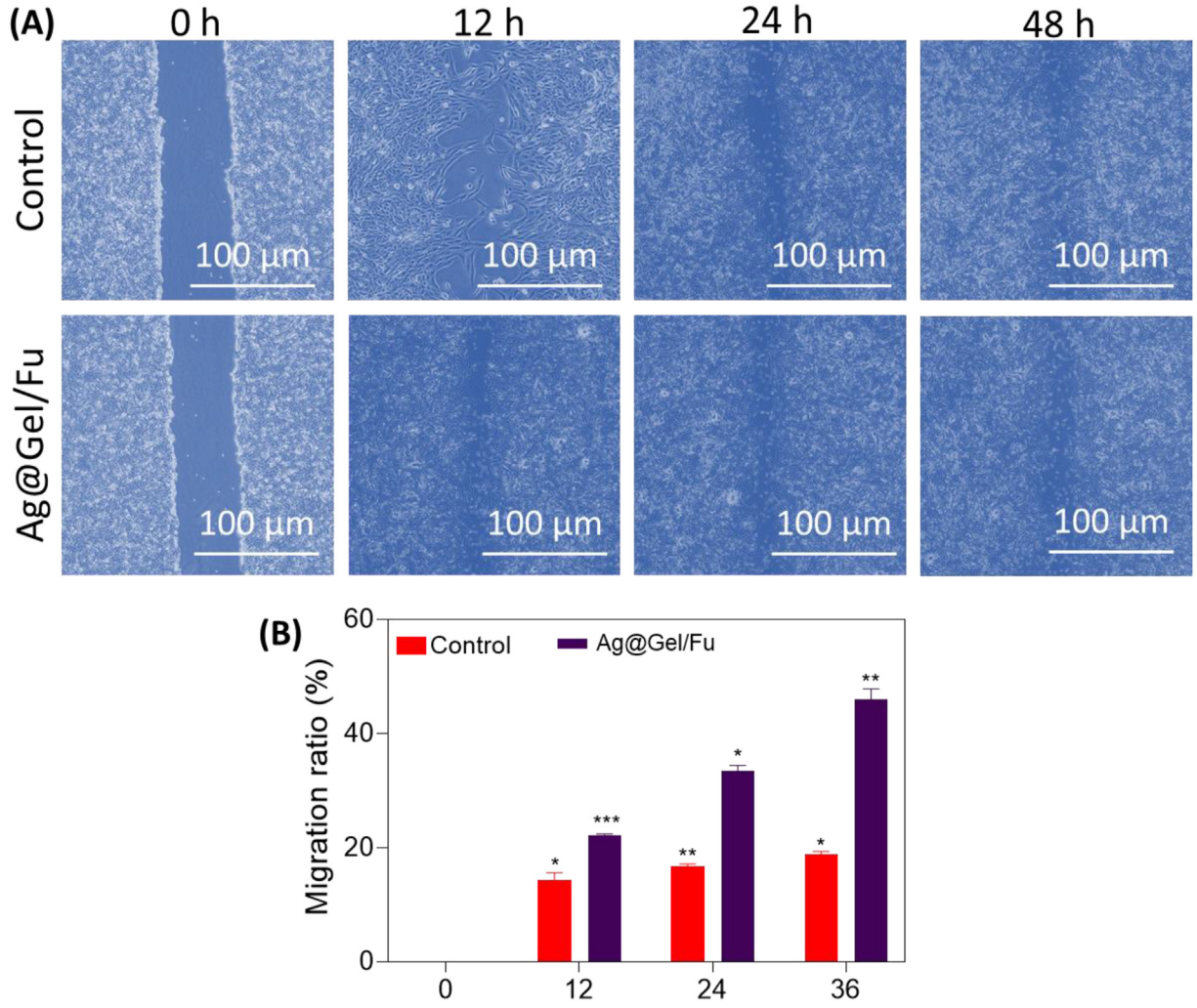

Fig. 8. (A&B) Cell migration area of L929 cells post-exposure of Ag@Gel/Fu in wound scratch assay and inverted phase contrast microscopic images. The scale bar indicates the 100 μm. Data were stated as means ± SEM (n = 5). *P < 0.05, **P < 0.01, ***P < 0.001, compared with control group (#).

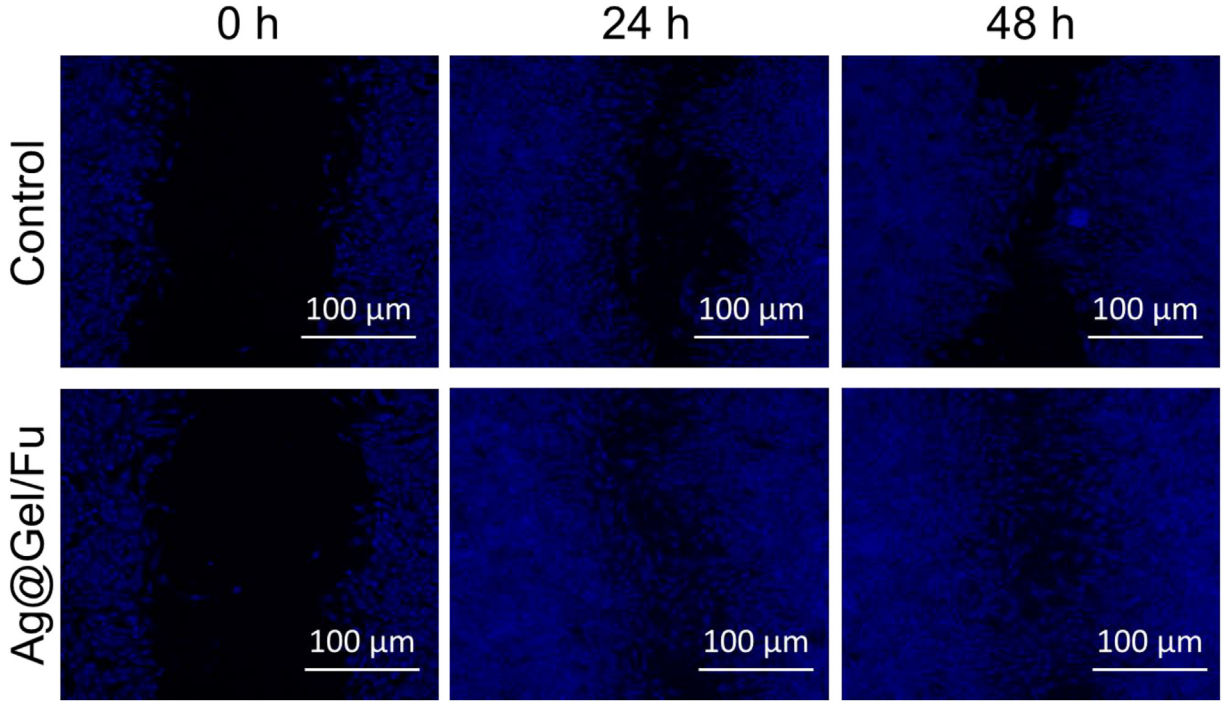

Fig. 9. Fluorescence microscopic images of L929 cells with DAPI staining in wound scratch assay. The scale bar indicates the 100 μm.

The overall cytotoxicity assay proved that Ag@Gel/Fu nanogel is highly suitable for nursing care wound healing nursing care treatment. Further, several studies have reported on the *in vitro* cytotoxicity of AgNPs in non-cancerous and cancerous cells in L929 cells [47].

3.8. Wound healing study

Many silver dressings are on the market, but the expenses are high. The dressings without silver possess poor antimicrobial properties. The wound-healing process of drugs has depended on collagen deposition and fibroblast formation in a wound site. The results of the wound scratch assay confirmed that excellent cell proliferation and migration were observed after 12 h of cell scratched area. The size of the wound closer was recorded at different time intervals of 0, 12, 24, and 48 h (Fig. 8A). The simultaneous release of the fucoidan and gelatin biomolecules triggered the protein secretion. The gelatine molecules can stimulate cell migration and healing (Fig. 8B). The fluorescence microscopic images of wound scratches show a significant enhancement in cell regeneration. In this case, the control cells are threefold higher. Ag@Gel/Fu nanogel exhibits uniform proliferation without microbial inflammation and death cells (Fig. 9). As a result of *in vitro* studies, the impact of Ag@Gel/Fu nanogel prominently enhances the efficacy of antibacterial-mediated wound healing nursing care in a short period. Ag@Gel/Fu nanogel has shown excellent biocompatibility in normal skin cells.

4. Conclusion

In summary, gelatin reduces and stabilizes Ag@Gel/Fu nanogel agents. Fucoidan was added to obtain a novel composition Ag@Gel/Fu, which enhanced the gelatin crosslinking. The amino and sulfur group of fucoidan formed a coordination bond with Ag@Gel/Fu, stabilizing the nanogel uniformity. The results of antibacterial and antibiofilm activity assays suggested that Ag@Gel/Fu nanogel effectively eradicates bacterial proliferation and biofilm-forming ability against wound-infecting pathogens. The better antibacterial effect of nanogel enabled the maintained wound area to remain clean and without infection. *In vitro* cytotoxicity studies indicated that Ag@Gel/Fu nanogel has excellent biocompatibility and can shorten the wound healing period. These research findings demonstrate that Ag@Gel/Fu nanogel is an antibacterial wound material that promotes the wound-healing nursing care process. Accordingly, it has promising wound-healing properties and should be considered in future clinical studies.

Contributions

All authors read and approved the final version of the manuscript. **Jiao Hao:** Conceptualization, Writing, Data curation, Software, Writing Original Draft, and Methodology. **Yaomiao Du:** Analyzed and Interpreted the Data, Resources, Contributed Reagents and Materials. **Yaomiao Du:** Conceptualization, Writing, Data curation, Analysis data, and Writing - Review & Editing.

Ethical approval

Not applicable.

Consent for publication

Not applicable.

Data availability statement

The data supporting this study's findings are available from the corresponding author upon reasonable request.

Fundings

Not applicable.

Declaration of competing interest

The authors declare that they have no known competing financial interests or personal relationships that could have appeared to influence the work reported in this paper.

References

[1] Wang C, Niu X, Bao S, Shen W, Jiang C. Distribution patterns and antibiotic resistance profiles of bacterial pathogens among patients with wound infections in the jiaxing region from 2021 to 2023. Infect Drug Resist 2024:2883–96.
[2] Mariani F, Galvan EM. Staphylococcus aureus in polymicrobial skinand soft tissue infections: impact of inter-species interactionsin disease outcome. Antibiotics 2023;12(7):1164.
[3] Kato T, Yanagiuchi T, Hirano K, Imura H, Matsubara K, Hanabusa K, et al. Impact of antimicrobial-resistant bacterial and polymicrobial infection on wound healing after minor forefoot amputation in chronic limb-threatening ischemia with infection. J Endovasc Ther 2024;31(3):450–6.
[4] Uberoi A, McCready-Vangi A, Grice EA. The wound microbiota: microbial mechanisms of impaired wound healing and infection. Nat Rev Microbiol 2024:1–15.
[5] Diban F, Di Lodovico S, Di Fermo P, D'Ercole S, D'Arcangelo S, Di Giulio M, et al. Biofilms in chronic wound infections: innovative antimicrobial approaches using the in vitro Lubbock chronic wound biofilm model. Int J Mol Sci 2023;24(2):1004.
[6] Fu W, Sun S, Cheng Y, Ma J, Hu Y, Yang Z, et al. Opportunities and challenges of nanomaterials in wound healing: advances, mechanisms, and perspectives. Chem Eng J 2024:153640.
[7] Cao Y, Sun J, Qin S, Zhou Z, Xu Y, Liu C. Advances and challenges in immunemodulatory biomaterials for wound healing applications. Pharmaceutics 2024;16(8):990.
[8] Ghaffari A, Abazari M, Moghimi HR. Wound healing and nanotechnology: opportunities and challenges. Bioengineered nanomaterials for wound healing and infection control. 2023. p. 115–74.
[9] Wang C, Niu X, Bao S, Shen W, Jiang C. Distribution patterns and antibiotic resistance profiles of bacterial pathogens among patients with wound infections in the jiaxing region from 2021 to 2023. Infect Drug Resist 2024:2883–96.
[10] Soldevila-Boixader L, Fernández AP, Laguna JM, Uçkay I. Local antibiotics in the treatment of diabetic foot infections: a narrative review. Antibiotics 2023;12:124. 2023.
[11] Zhou C, Zou Y, Xu R, Han X, Xiang Z, Guo H, …, Sun Y. Metal-phenolic self-assembly shielded probiotics in hydrogel reinforced wound healing with antibiotic treatment. Mater Horiz 2023;10(8):3114–23.
[12] Lu Y, Li J. The outcome of prolonged postoperative antibiotics on wound healing in orthognathic surgery: a meta-analysis. Int Wound J 2023;20(6):2233–40.
[13] Valentino C, Martinez Rodriguez T, Borrego-Sanchez A, Hernandez Benavides P, Arrebola Vargas F, Paredes JM, et al. Characterization and molecular modelling of non-antibiotic nanohybrids for wound healing purposes. Pharmaceutics 2023;15(4):1140.
[14] Liu Y, Tan L, Huang Y, Chen M, Li M, Cai K, et al. Multifunctional antibiotics-free hydrogel dressings with self-regulated nitric oxide-releasing kinetics for improving open wound healing. J Mater Chem B 2023;11(16):3650–68.
[15] Chen P, Vilorio NC, Dhatariya K, Jeffcoate W, Lobmann R, McIntosh C, et al. Guidelines on interventions to enhance healing of foot ulcers in people with diabetes (IWGDF 2023 update). Diabetes Metabol Res Rev 2024;40(3):e3644.
[16] Kumar P, Hasan F, Kumar V, Chawla R, Goyal SK. Diabetic wound healing: navigating physiology, advancements and research frontiers. J Dia Res Rev Rep SRC/JDRR-202 2024;181(6):2–11. https://doi.org/10.47363/JDRR/2024.
[17] Norahan MH, Pedroza-Gonzalez SC, Sanchez-Salazar MG, Álvarez MM, de Santiago GT. Structural and biological engineering of 3D hydrogels for wound healing. Bioact Mater 2023;24:197–235.
[18] Che L, Wang P, Ma L, Feng Y, Zhao J, Li X. A simulation analysis method for strength and fatigue design of prestressed wound ultra-high-pressure vessels. Adv Mech Eng 2023;15(11):16878132231209640.
[19] Huang F, Lu X, Yang Y, Yang Y, Li Y, Kuai L, et al. Microenvironment-based diabetic foot ulcer nanomedicine. Adv Sci 2023;10(2):2203308.
[20] Perez-Diaz MA, Prado-Prone G, Diaz-Ballesteros A, Gonzalez-Torres M, Silva-Bermudez P, Sanchez-Sanchez R. Nanoparticle and nanomaterial involvement

during the wound healing process: an update in the field. J Nanoparticle Res 2023;25(2):27.
[21] Gowda BHJ, Mohanto S, Singh A, Bhunia A, Abdelgawad MA, Ghosh S, et al. Nanoparticle-based therapeutic approaches for wound healing: a review of the state-of-the-art. Mater Today Chem 2023;27:101319.
[22] Sari MHM, Cobre ADF, Pontarolo R, Ferreira LM. Status and future scope of soft nanoparticles-based hydrogel in wound healing. Pharmaceutics 2023;15(3):874.
[23] Froelich A, Jakubowska E, Wojtyłko M, Jadach B, Gackowski M, Gadzinski P, et al. Alginate-based materials loaded with nanoparticles in wound healing. Pharmaceutics 2023;15(4):1142.
[24] Aldakheel FM, Mohsen D, El Sayed MM, Alawam KA, Binshaya AS, Alduraywish SA. Silver nanoparticles loaded on chitosan-g-PVA hydrogel for the wound-healing applications. Molecules 2023;28(7):3241.
[25] Rybka M, Mazurek Ł, Konop M. Beneficial effect of wound dressings containing silver and silver nanoparticles in wound healing from experimental studies to clinical practice. Life 2022;13(1):69.
[26] Vijayakumar G, Kim HJ, Rangarajulu SK. In vitro antibacterial and wound healing activities evoked by silver nanoparticles synthesized through probiotic bacteria. Antibiotics 2023;12(1):141.
[27] Jangid H, Singh S, Kashyap P, Singh A, Kumar G. Advancing biomedical applications: an in-depth analysis of silver nanoparticles in antimicrobial, anticancer, and wound healing roles. Front Pharmacol 2024;15:1438227.
[28] Mohammed HA, Amin MA, Zayed G, Hassan Y, El-Mokhtar M, Saddik MS. In vitro and in vivo synergistic wound healing and anti-methicillin-resistant Staphylococcus aureus (MRSA) evaluation of liquorice-decorated silver nanoparticles. J Antibiot 2023;76(5):291–300.
[29] Aldakheel FM, Sayed MME, Mohsen D, Fagir MH, El Dein DK. Green synthesis of silver nanoparticles loaded hydrogel for wound healing; systematic review. Gels 2023;9:530. 2023.
[30] Alavi M, Varma RS. Antibacterial and wound healing activities of silver nanoparticles embedded in cellulose compared to other polysaccharides and protein polymers. Cellulose 2021;28(13):8295–311.
[31] Borhani M, Dadpour S, Haghighizadeh A, Etemad L, Soheili V, Memar B, et al. Crosslinked hydrogel loaded with chitosan-supported iron oxide and silver nanoparticles as burn wound dressing. Pharmaceut Dev Technol 2023;28(10):962–77.
[32] Sethi S, Saruchi Medha, Thakur S, Kaith BS, Sharma N, Kuma V. Biopolymer starch-gelatin embedded with silver nanoparticle-based hydrogel composites for antibacterial application. Bio Con Bio 2022;12(11):5363–84.
[33] Talodthaisong C, Patramanon R, Thammawithan S, Lapmanee S, Maikaeo L, Sricharoen P, et al. A shear-thinning, self-healing, dual-cross linked hydrogel based on gelatin/vanillin/Fe3+/AGP-AgNPs: synthesis, antibacterial, and wound-healing assessment. Macromol Biosci 2023;23(12):2300250.
[34] Li T, Yang J, Weng C, Liu P, Huang Y, Meng S, et al. Intra-articular injection of anti-inflammatory peptide-loaded glycol chitosan/fucoidan nanogels to inhibit inflammation and attenuate osteoarthritis progression. Int J Biol Macromol 2021;170:469–78.
[35] Ohmes J, Mikkelsen MD, Nguyen TT, Tran VHN, Meier S, Nielsen MS, et al. Depolymerization of fucoidan with endo-fucoidanase changes bioactivity in processes relevant for bone regeneration. Carbohydr Polym 2022;286:119286.
[36] Younas A, Dong Z, Hou Z, Asad M, Li M, Zhang N. A chitosan/fucoidan nanoparticle-loaded pullulan microneedle patch for differential drug release to promote wound healing. Carbohydr Polym 2023;306:120593.
[37] Tarbeeva DV, Krylova NV, Iunikhina OV, Likhatskaya GN, Kalinovskiy AI, Grigorchuk VP, et al. Biologically active polyphenolic compounds from Lespedeza bicolor. Fitoterapia 2022;157:105121.
[38] Ambli M, Deracinois B, Ravallec R, Cudennec B, Flahaut C. Gelatine, present use and future applications: decryption of a high-value multi-purpose by-product of the agro-food industry. J Food Sci Nutri Res 2023;6(4).
[39] Alfei S, Giordani P, Zuccari G. Synthesis and physicochemical characterization of gelatine-based biodegradable aerogel-like composites as possible scaffolds for regenerative medicine. Int J Mol Sci 2024;25(9):5009.
[40] Rosli NSM, Ahmed S, Sarbon NM. Gelatin alternative: extractability and functional and bioactivity properties. In: Natural gums. Elsevier; 2023. p. 507–51.
[41] Andreazza R, Morales A, Pieniz S, Labidi J. Gelatin-based hydrogels: potential biomaterials for remediation. Polymers 2023;15(4):1026.
[42] Yu H, Zhang Q, Farooqi AA, Wang J, Yue Y, Geng L, et al. Opportunities and challenges of fucoidan for tumors therapy. Carbohydr Polym 2023:121555.
[43] Dubashynskaya NV, Gasilova ER, Skorik YA. Nano-sized fucoidan inter polyelectrolyte complexes: recent advances in design and prospects for biomedical applications. Int J Mol Sci 2023;24(3):2615.
[44] George A, Shrivastav PS. Fucoidan, a brown seaweed polysaccharide in nano drug delivery. Drug Deliv Trans Res 2023;13(10):2427–46.
[45] Raju P, Arivalagan P, Natarajan S. One-pot fabrication of multifunctional catechin@ ZIF-L nanocomposite: assessment of antibiofilm, larvicidal and photocatalytic activities. J Photochem Photobiol B Biol 2020;203:111774.
[46] Dhaka A, Mali SC, Sharma S, Trivedi R. A review on biological synthesis of silver nanoparticles and their potential applications. Results in Chemistry 2023;6:101108.
[47] Basavarajappa DS, Kumar RS, Almansour AI, Chakraborty B, Bhat MP, Nagaraja SK, et al. Biofunctionalized silver nanoparticles synthesized from Passiflora vitifolia leaf extract and evaluation of its antimicrobial, antioxidant and anticancer activities. Biochem Eng J 2022;187:108517.